Eur. Phys. J. A **31**, 409–414 (2007)
DOI 10.1140/epja/i2006-10163-0

THE EUROPEAN PHYSICAL JOURNAL A

Special Article – QNP 2006

Neutrino-nucleus interactions

T.W. Donnelly[a]

Center for Theoretical Physics, Laboratory for Nuclear Science and Department of Physics, Massachusetts Institute of Technology, Cambridge, MA 02139, USA

Received: 24 September 2006
Published online: 16 February 2007 –

Abstract. Inclusive electron scattering cross-sections in the quasielastic and resonance regions for few GeV electrons are well represented in terms of scaling functions and scaling variables, the so-called superscaling analysis (SuSA). The concepts of scaling of the first and second kinds and superscaling are discussed, as are several mechanisms which are known to yield scaling violations. Given the high quality of scaling for cross-sections at appropriate kinematics, it is shown how the ideas can be turned around to provide predictions for both charge-changing and neutral current neutrino reactions with nuclei at comparable kinematics.

PACS. 23.40.Bw Weak-interaction and lepton (including neutrino) aspects – 24.10.Jv Relativistic models – 25.30.-c Lepton-induced reactions – 25.30.Fj Inelastic electron scattering to continuum

1 Scaling of the first kind

A basic contention in the present discussions is the following: While it may not be sufficient, it is necessary that in modeling electroweak interactions with nuclei at few GeV energies a good understanding of existing inclusive electron scattering data must be reached before one can have much confidence in predictions of neutrino reactions with nuclei. Presently, modeling is not completely able to provide good enough understanding, and consequently other approaches must also be pursued. In particular, the approach followed here uses concepts of scaling [1–14] (0th, 1st and 2nd kinds and superscaling: the superscaling analysis, SuSA).

For inclusive semi-leptonic electroweak processes, in addition to the lepton scattering angle, one has energy transfer ω and 3-momentum transfer q (or, equivalently, Q^2 and ν). First, one replaces ω with the scaling variable $y = y(q,\omega)$, given by the lowest value of the missing momentum at the lowest missing energy kinematically allowed for semi-inclusive knockout of nucleons from the nucleus. While an exact formula can be written [1], the following is a reasonable approximation [2,3] for the y-scaling variable:

$$y = y(q,\omega) \cong \sqrt{\tilde{\omega}(2m_N + \tilde{\omega})} - q\,,$$

where $\tilde{\omega} \equiv \omega - E_s$ with E_s the separation energy and m_N the nucleon mass. This choice is motivated by the understanding that the main contributions to quasielastic (QE) inclusive electroweak cross-sections arise from the above kinematic region, making y play a special role.

Second, one defines the function

$$F(q,y) \equiv \frac{\mathrm{d}^2\sigma/\mathrm{d}\Omega_e\mathrm{d}\omega}{A\Sigma_{eN}^{eff}}\,,$$

where the numerator is the double-differential inclusive electron scattering cross-section and the denominator

$$A\Sigma_{eN}^{eff} = Z\overline{\sigma}_{ep}^{elastic} + N\overline{\sigma}_{en}^{elastic}$$

is proportional to the effective (*i.e.*, incorporating relativistic effects; see [2,3]) single-nucleon cross-section with proton and neutron numbers as weighting factors. Typical results are shown in fig. 1 (and more may be found in [1]). As the momentum transfer becomes very large one sees that the results become independent of q and therefore $F(q,y)$ tends towards a universal function which depends only on the scaling variable

$$F(q,y) \to F(y) \equiv F(\infty,y);$$

one calls this behavior *scaling of the 1st kind*. Note that in the region above the QE peak ($y \cong 0$) where resonances, meson production and the start of Deep Inelastic Scattering (DIS) enter, 1st-kind scaling is, not unexpectedly, badly violated.

[a] e-mail: donnelly@mit.edu

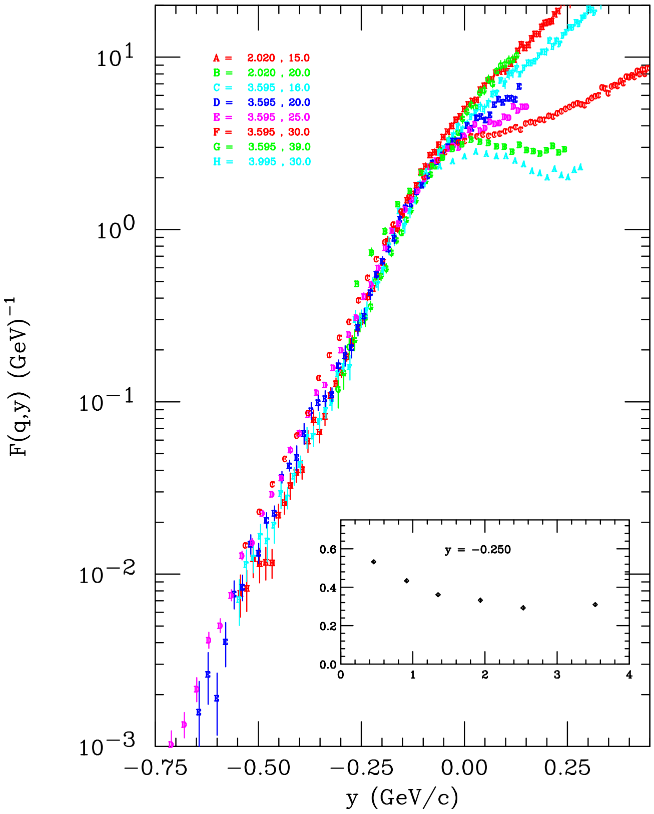

Fig. 1. Scaling of the 1st kind in ^{56}Fe. The various data sets correspond to different beam energies and scattering angles, and therefore to different values of momentum transfer. The inset shows the approach to scaling as a function of q at $y = -0.25$. See [1] for references to the data.

2 Scaling of the second kind

Next, one introduces a characteristic momentum scale for a given nuclear species

$$k_A = \sqrt{\langle k^2 \rangle_A}$$

and uses this to define a dimensionless function

$$f(q,y) \equiv k_A \cdot F(q,y).$$

Correspondingly, one wishes to introduce a dimensionless scaling variable ψ and then to plot $f(q,\psi)$ *versus* ψ for fixed kinematics but different nuclear species. The Relativistic Fermi Gas (RFG) model [4] is used to motivate the choice of the scaling variable. In the RFG one has

$$[k_A]^{RFG} = k_F$$

and the dimensionless RFG scaling variable is given by

$$\begin{aligned}\psi &= \frac{1}{\sqrt{\xi_F}} \frac{\lambda - \tau}{\sqrt{(1+\lambda)\tau + \kappa\sqrt{\tau(1+\tau)}}} \\ &\cong \frac{1}{\eta_F}\left[\lambda\sqrt{1+1/\tau} - \kappa\right] \\ &\cong y/k_A\,,\end{aligned}$$

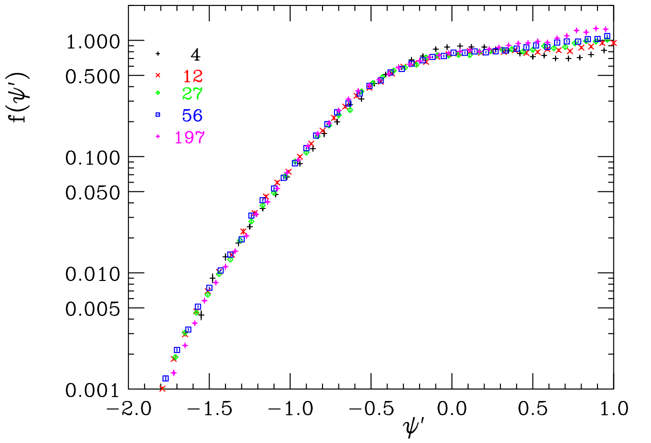

Fig. 2. Scaling of the 2nd kind at 3.6 GeV beam energy and a scattering angle of 16 degrees for nuclei ranging from ^{4}He to ^{197}Au. See [2,3] for references to the data.

where $\kappa \equiv q/2m_N$, $\lambda \equiv \omega/2m_N$, $\tau \equiv |Q^2|/4m_N^2 = \kappa^2 - \lambda^2 > 0$, $\eta_F \equiv k_F/m_N \sim 0.25$ and $\xi_F \equiv \sqrt{1+\eta_F^2} - 1 \cong \eta_F^2/2 \sim 0.03$. In performing detailed analyses of data, the scaling variable actually used is denoted ψ' and has a small empirical shift in energy loss, E_{shift}, in going from ω to $\omega - E_{shift}$ in the above expressions.

The results are displayed in fig. 2. In the scaling region ($\psi' < 0$) a universal behavior is seen, with very little dependence on the nuclear species; that is, one observes *scaling of the 2nd kind*. Again, in the region above $\psi' = 0$ where resonances, meson production and the start of DIS enter the 2nd-kind scaling is not as good (see the discussions in sect. 4, however).

3 Superscaling

Although the amount of data separated into longitudinal (L) and transverse (T) responses is small, one can attempt a scaling analysis with what does exist. The inclusive cross-section may be written

$$\frac{\mathrm{d}^2\sigma}{\mathrm{d}\Omega_e \mathrm{d}\omega} = \sigma_M \left[v_L R_L(q,\omega) + v_T R_T(q,\omega)\right],$$

where $v_L = |Q^2/q^2|^2$ and $v_T = \frac{1}{2}|Q^2/q^2| + \tan^2\theta_e/2$ are the usual Rosenbluth factors for inclusive electron scattering and σ_M is the Mott cross-section. From the individual response functions one can define corresponding scaling functions:

$$\begin{aligned}F_{L,T}(q,y) &\equiv \frac{R_{L,T}(q,\omega)}{\left[A\Sigma_{eN}^{eff}\right]_{L,T}/\sigma_M v_{L,T}}\,, \\ f_{L,T}(q,y) &\equiv k_A \cdot F_{L,T}(q,y)\,.\end{aligned}$$

Let us focus on the longitudinal scaling function. In contrast to the transverse sector, here one does not expect large contributions from either meson-exchange currents (MEC) and their associated correlations [6–8] or inelastic

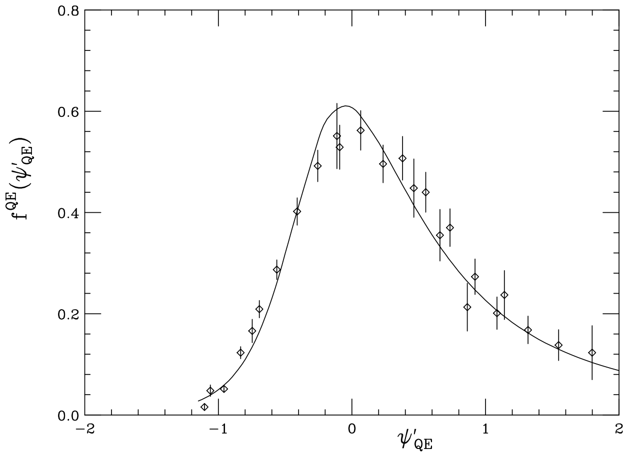

Fig. 3. Longitudinal scaling function from the analysis in [15], together with a parametrized fit from [5].

contributions from pion production and electroproduction of resonances such as the Δ (for example, see [9] for further discussions). Accordingly, the longitudinal scaling function provides a unique window into the roles played by the nuclear dynamics, both from initial-state energy and momentum distributions and from final-state interaction effects.

What results for the longitudinal scaling function is shown in fig. 3 where data together with a parametrization are shown plotted *versus* the scaling variable (which is now denoted ψ'_{QE} to emphasize the fact that it builds in the kinematics of elastic eN scattering, but no inelasticity as in the following section). This is seen to be both independent of q (scaling of the 1st kind) and also independent of nuclear species (scaling of the 2nd kind); that is, one has *superscaling*. These phenomenological results should be compared with the RFG model where the scaling function is given by a parabola which lies in the range $-1 < \psi'_{QE} < +1$ and peaks at the value 0.75. Clearly the RFG, while roughly correct, is not so in detail: the peak value is about 25% too high and the scaling function is symmetrical, whereas the experimental one has a pronounced asymmetry with a tail extending to high-energy loss (positive scaling variable). In recent modeling this behavior has also been observed in some cases [10,11] and appears to occur only when relatively strong final-state interactions are present.

Furthermore, in the RFG one has

$$[f_L]^{RFG} = [f_T]^{RFG} = [f]^{RFG}$$

which has been called *scaling of the 0th kind*. Indeed, if it were not for contributions from resonances, meson production and DIS (which should not scale, since they involve different elementary cross-sections, not elastic eN scattering, and since the scaling variables constructed above are appropriate only for QE scattering; see the discussions to follow), and for effects from MEC and their associated correlations one would expect scaling of the 0th kind to be found. In recent modeling [10–14] this behavior has been verified.

4 Scaling in the resonance region

In recent work [12] the resonance region has been studied as well as the QE region. First, the QE scaling variable introduced above must be replaced by a new one when, instead of eN elastic scattering, one excites the nucleon to a resonance of mass m_*:

$$\psi \to \psi_* = \frac{1}{\sqrt{\xi_F}} \frac{\lambda - \tau\rho_*}{\sqrt{(1+\lambda\rho_*)\tau + \kappa\sqrt{\tau(1+\tau\rho_*^2)}}} ,$$

where $\rho_* \equiv 1 + (m_*^2 - m_N^2)/|Q^2| \geq 1$ (and $\rho_* = 1$ for elastic, *i.e.*, QE, scattering). As above, ψ'_* is defined using the same expression, but with the energy shift E_{shift}.

Second, the fact that the elementary cross-section is not that of elastic eN scattering has to be taken into account. One begins by writing the inclusive cross-section in the form

$$\frac{\mathrm{d}^2\sigma}{\mathrm{d}\Omega_e \mathrm{d}\omega} \equiv \Sigma^{QE} + \Sigma' ,$$

namely, into a piece that is called quasielastic and is assumed to obey scaling of the 0th kind, plus a piece that contains the remaining contributions. The QE piece is thus assumed to be

$$\Sigma^{QE} \equiv \frac{A\Sigma_{eN}^{eff}}{k_A} \cdot f_L(\psi'_{QE}) ,$$

i.e., it employs the *longitudinal* scaling function for both L and T contributions to the cross-section. The remainder, Σ', should then contain (at least) the contributions from inelastic eN scattering and MEC+correlation effects.

As a first approximation in [12] it was assumed that the dominant effect in the 1 GeV regime is from electroexcitation of the Δ, and that MEC+correlation effects, while not absent, are corrections to this. One then proceeds as follows: first, the QE contribution (called $[\Sigma^{QE}]_{expt}$, since the experimental scaling function was used) is subtracted from the total experimental cross-section to isolate the remainder:

$$[\Sigma']_{expt} = \left[\frac{\mathrm{d}^2\sigma}{\mathrm{d}\Omega_e \mathrm{d}\omega}\right]_{expt} - \left[\Sigma^{QE}\right]_{expt} .$$

Second, following the approach pursued in [12], one makes the assumption that the next most important contribution in this range of kinematics arises from electroproduction of the Δ. Of course this is only a rough approximation, since non-resonant pion production, the tails of other resonances or, alternatively, contributions from DIS are not totally absent; likewise MEC effects with their associated correlations can also play a role. However, the Δ is certainly important and, accordingly, the analysis proceeded by invoking dominance of this mode, implying that the remainder is to be divided by the effective $N \to \Delta$ electron scattering cross-section to define a new function

$$F^{\Delta}(q, y) \equiv \frac{[\Sigma']_{expt}}{A\Sigma_{N\Delta}^{eff}} ,$$

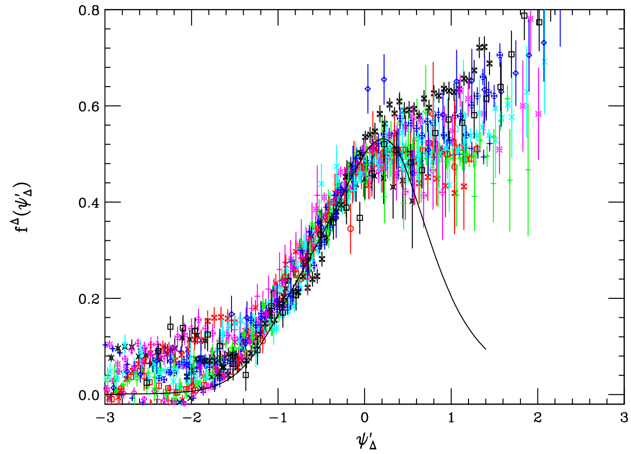

Fig. 4. Scaling in the resonance region (see text for discussion).

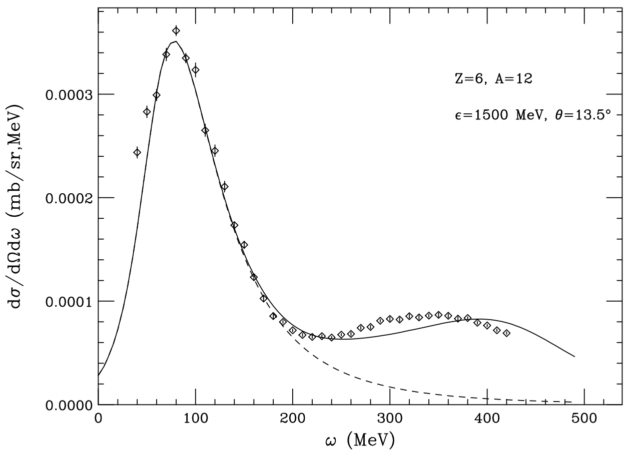

Fig. 5. Inclusive electron scattering from ^{12}C at beam energy 1.5 GeV and scattering angle 13.5 degrees, together with the results of using the phenomenological scaling functions discussed in the text.

where

$$A\Sigma^{eff}_{N\Delta} = Z\overline{\sigma}^{inelastic}_{p\to\Delta^+} + N\overline{\sigma}^{inelastic}_{n\to\Delta^0}\,.$$

As before, a dimensionless scaling function may also be defined:

$$f^{\Delta}(q,y) \equiv k_A \cdot F^{\Delta}(q,y)\,.$$

The results are then plotted in fig. 4 as a function of an inelastic scaling variable which in this initial analysis has been constructed using the centroid mass of the Δ, also an approximation:

$$\psi'_{\Delta} \equiv \psi'_{*}(m_{*} \to m_{\Delta})\,.$$

Rather good scaling behavior is observed in the region below the Δ peak where $\psi'_{\Delta} = 0$, although, as expected, not at higher-energy loss where higher-lying resonances, DIS, etc., take over. In the region below the Δ peak there is some residual which is presumably at least partially due to effects from MEC and their associated correlations.

This means that one should have a reasonable representation of the total inclusive electron scattering cross-section for the 1 GeV energy regime for energies ranging

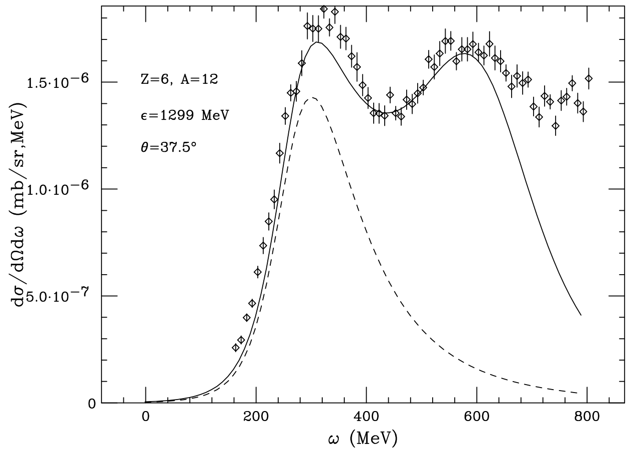

Fig. 6. As for the previous figure, but now at beam energy 1.3 GeV and scattering angle 37.5 degrees.

from below the QE peak (typically around $\psi'_{\Delta} \sim -1$ in fig. 4) up through the peak of the Δ. To test this one can reassemble the complete inclusive cross-section using the QE and Δ scaling functions with their attendant single-baryon cross-sections. Typical results are shown in figs. 5 and 6. Clearly, one has a rather successful understanding of the EM inclusive cross-section for this range of kinematics, leaving a residual typically of perhaps 10–15% to be accounted for by effects likely from MEC and their associated correlations.

5 Neutrino-nuclear cross-sections

Just as for the electron scattering reactions in the QE and Δ regions, the scaling functions determined above are employed, but now multiplied by the corresponding charge-changing (CC) neutrino reaction cross-sections for the Z protons and N neutrons in the nucleus. The CCν cross-section may be written:

$$\left[\frac{\mathrm{d}^2\sigma}{\mathrm{d}\Omega_{kk'}\,\mathrm{d}k'}\right]_{\chi} = \sigma_0 R_{\chi}\,,$$

where

$$\sigma_0 \equiv \frac{(G\cos\theta_c)^2}{2\pi^2}\left[k'\cos\widetilde{\theta}_{kk'}\right]^2$$

is the elementary cross-section (the analog of the Mott cross-section in sect. 3) containing the Cabibbo angle θ_c, the charged lepton momentum k' and an effective scattering angle $\theta_{kk'}$ defined via

$$\tan^2\widetilde{\theta}_{kk'} \equiv \frac{|Q^2|}{4\epsilon\epsilon' - |Q^2|}\,,$$

where ϵ and ϵ' are the incident neutrino and final-state charged lepton energies, respectively. The subscript $\chi = +(-)$ labels the specific case, *i.e.*, neutrinos (antineutrinos). The response function above may be decomposed into individual angle-independent responses, just as when

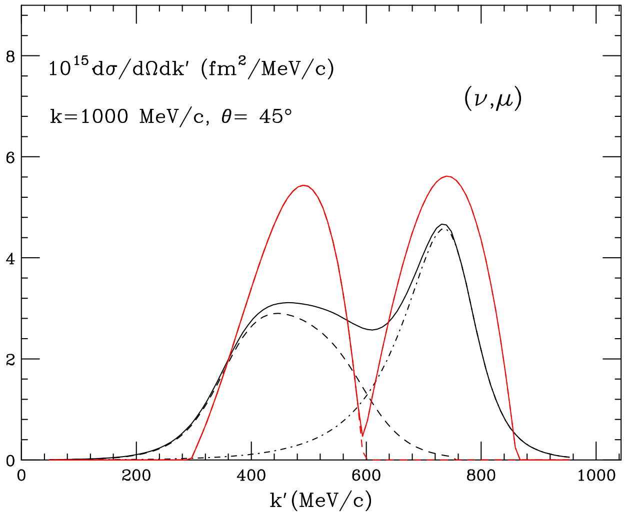

Fig. 7. Charge-changing muon neutrino cross-sections at neutrino energy $k = 1\,\mathrm{GeV}$ and scattering angle 45 degrees. The right-hand peaks are from QE contributions while the left-hand ones are from the Δ. The upper curves are obtained using the RFG, while the lower ones are using the phenomenological scaling analysis.

discussing inclusive electron scattering. This time, since there is a vector (V)/axial-vector (A) parity-violating interference and since the axial-vector current is not conserved, one has more terms:

$$R_\chi = \left[\widehat{V}_{CC}R_{CC} + 2\widehat{V}_{CL}R_{CL} + \widehat{V}_{LL}R_{LL} + \widehat{V}_T R_T\right] + \chi\left[\widehat{V}_{T'}R_{T'}\right],$$

where $R_K = R_K^{VV} + R_K^{AA}$ for $K = CC$, CL, LL, T and R_K^{VA} for $K = T'$. The various contributions are labeled with C for charge, L for longitudinal and T or T' for the two types of transverse responses which can enter. The kinematic factors $\widehat{V}_K$ are generalizations of the familiar Rosenbluth factors given in sect. 3 which account for the finite mass of the charged lepton (see [12] for specifics). For charge-changing muon neutrino processes in the QE region one has the elementary reactions $\nu_\mu + n \to p + \mu^-$ and $\overline{\nu}_\mu + p \to n + \mu^+$, while in the Δ region one has $\nu_\mu + p \to \Delta^{++} + \mu^-$, $\nu_\mu + n \to \Delta^+ + \mu^-$, $\overline{\nu}_\mu + p \to \Delta^0 + \mu^+$ and $\overline{\nu}_\mu + n \to \Delta^- + \mu^+$.

Typical results are shown in fig. 7. The two peaks are from QE (right) and Δ (left) regions, with the higher-lying curves for the RFG and the lower-lying from the phenomenological scaling analyses. Clearly, there are significant differences and, while providing a rough measure of the electroweak responses, the RFG results are higher and more localized than the SuSA results. Although not shown here, it should be noted that non-relativistic approximations to the kinematics and electroweak currents yield cross-sections that are even further from the SuSA curves in fig. 7.

6 Conclusions and discussion

Several conclusions emerge from the SuSA approach presented here:

- Scaling of the 1st and 2nd kinds for inclusive electron scattering appears to be well satisfied at the QE peak and below (the scaling region); the region above the QE peak clearly has contributions which do not scale, at least in the same way as the QE cross-sections do. These scaling violations are at least partially due to inelastic processes such as electroexcitation of the Δ.
- For the longitudinal response superscaling is observed, as expected, since this response sector has only relatively small contributions from Δ production and from MEC effects.
- In recent work [12] these ideas have been extended into the Δ region. In that approach the QE contributions were subtracted and the remainder analyzed in terms of a Δ-dominated scaling function and scaling variable; again good scaling is seen.
- The SuSA approach has been used to make predictions for charge-changing neutrino reactions in the few GeV energy region. Significant differences are observed with respect to conventional RFG modeling.

In on-going studies the scaling ideas are being extended in several ways:

- A relativized shell model study of neutrino reactions was undertaken [13], yielding successful scaling behavior.
- A relativistic impulse approximation study of the superscaling function was undertaken in [10,11]. What was found is that the universal superscaling function arises naturally from relativistic mean-field modeling, although not from the relativistic plane-wave impulsive approximation (RPWIA) or from modeling which employs the real parts of conventional optical potentials.
- 1p-1h MEC/correlation effects have been explored in detail in [6], while 2p-2h MEC/correlation effects are presently being incorporated in relativistic modeling of EW processes [7,8]. Although the latter study has not yet been fully executed, the expectation is that 10–15% of the transverse EM response in the region between the QE peak and the Δ peak could be due to such effects. These contributions enter as scaling violating effects. One should also note an asymmetric feature of the MEC effects: in the transverse contributions, which are dominant for neutrino reactions in the 1 GeV energy regime, the MEC contribute to the vector current, but not in leading order to the axial-vector current. Hence, it is necessary to understand such effects when attempting to model the neutrino reaction cross-sections to better than 10–15%.
- Extensions to neutral-current (NC) neutrino scattering in the QE region (u-channel inclusive *versus* t-channel inclusive) have been undertaken [14]. Further extensions to include NC processes in the Δ region are being contemplated, as are both CCν and NCν reactions at higher inelasticity than the Δ region.

This work is supported by the U.S. Department of Energy (DOE) under cooperative agreement No. DE-FC02-94ER40818.

References

1. D.B. Day, J.S. McCarthy, T.W. Donnelly, I. Sick, Annu. Rev. Nucl. Part. Sci. **40**, 357 (1990).
2. T.W. Donnelly, I. Sick, Phys. Rev. Lett. **82**, 3212 (1999).
3. T.W. Donnelly, I. Sick, Phys. Rev. C **60**, 065502 (1999).
4. W.M. Alberico, A. Molinari, T.W. Donnelly, E. Kronenberg, J.W. Van Orden, Phys. Rev. C **38**, 1801 (1988).
5. C. Maieron, T.W. Donnelly, I. Sick, Phys. Rev. C **65**, 025502 (2002).
6. J.E. Amaro, M.B. Barbaro, J.A. Caballero, T.W. Donnelly, A. Molinari, Phys. Rep. **368**, 317 (2002) and references therein.
7. A. De Pace, M. Nardi, W.M. Alberico, T.W. Donnelly, A. Molinari, Nucl. Phys. A **726**, 303 (2003).
8. A. De Pace, M. Nardi, W.M. Alberico, T.W. Donnelly, A. Molinari, Nucl. Phys. A **741**, 249 (2004).
9. M.B. Barbaro, J.A. Caballero, T.W. Donnelly, C. Maieron, Phys. Rev. C **69**, 035502 (2004).
10. J.A. Caballero, J.E. Amaro, M.B. Barbaro, T.W. Donnelly, C. Maieron, J.M. Udias, Phys. Rev. Lett. **95**, 252502 (2005).
11. J.A. Caballero, Phys. Rev. C **74**, 015502 (2006).
12. J.E. Amaro, M.B. Barbaro, J.A. Caballero, T.W. Donnelly, A. Molinari, I. Sick, Phys. Rev. C **71**, 015501 (2005).
13. J.E. Amaro, M.B. Barbaro, J.A. Caballero, T.W. Donnelly, C. Maieron, Phys. Rev. C **71**, 065501 (2005).
14. J.E. Amaro, M.B. Barbaro, J.A. Caballero, T.W. Donnelly, Phys. Rev. C **73**, 035503 (2006).
15. J. Jourdan, Nucl. Phys. A **603**, 117 (1996).